



Geostatistical assessment of groundwater arsenic contamination in the Padana Plain

Massimiliano Schiavo^a, Beatrice M.S. Giambastiani^b, Nicolas Greggio^b, Nicolò Colombani^{c,*}, Micòl Mastrocicco^d

^a Department of Land, Environment, Agriculture, and Forestry (TESAF), University of Padova, Via dell'Università 16, 35020 Legnaro, (PD), Italy

^b Department of Biological, Geological and Environmental Sciences (BiGeA) at Interdepartmental Centre for Environmental Sciences Research (CIRSA), Alma Mater Studiorum University of Bologna, Via S. Alberto 163, 48123 Ravenna, Italy

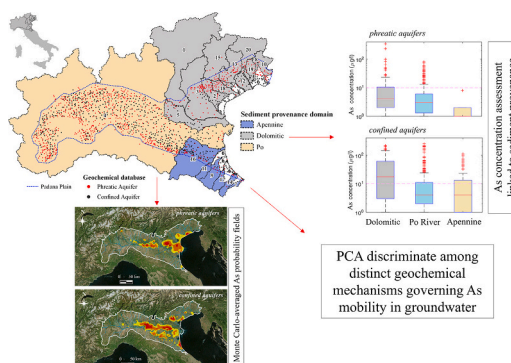
^c Department of Materials, Environmental Sciences and Urban Planning (SIMAU), Marche Polytechnic University, Via Breccie Bianche 12, 60131 Ancona, Italy

^d Department of Environmental, Biological and Pharmaceutical Sciences and Technologies (DiSTABiF), Campania University "Luigi Vanvitelli", Via A. Vivaldi 43, 81100 Caserta, Italy

HIGHLIGHTS

- Monte Carlo framework to assess As contamination & origins in Padana Plain aquifers
- Mixed oxic and reducing conditions in shallow aquifers limited the As mobility
- As release driven by reductive dissolution of Mn and Fe-oxides, SOM mineralization
- The most vulnerable areas have sediments with fluvio-glacial or dolomitic origins.

GRAPHICAL ABSTRACT



ARTICLE INFO

Editor: Jurgen Mahlknecht

Keywords:

Metalloid pollution
Monte Carlo approach
PCA
Groundwater quality
Aquifer matrix
Redox processes

ABSTRACT

Arsenic (As) in groundwater from natural and anthropogenic sources is one of the most common pollutants worldwide affecting people and ecosystems. A large dataset from >3600 wells is employed to spatially simulate the depth-averaged As concentration in phreatic and confined aquifers of the Padana Plain (Northern Italy). Results of in-depth geostatistical analysis via PCA and simulations within a Monte Carlo framework allow the understanding of the variability of As concentrations within the aquifers. The most probable As contaminated zones are located along the piedmont areas in the confined aquifers and in the lowland territories in the phreatic aquifers. The distribution of the As contaminated zones has been coupled with hydrogeological, geological, and geochemical information to unravel the sources and mechanisms of As release in groundwater. The reductive dissolution of Fe oxyhydroxides and organic matter mineralization under anoxic conditions resulted to be the major drivers of As release in groundwater. This phenomenon is less evident in phreatic aquifers, due to mixed oxic and reducing conditions. This large-scale study provides a probabilistic perspective on As contamination, e.

* Corresponding author.

E-mail address: n.colombani@univpm.it (N. Colombani).

<https://doi.org/10.1016/j.scitotenv.2024.172998>

Received 13 January 2024; Received in revised form 29 March 2024; Accepted 2 May 2024

Available online 5 May 2024

0048-9697/© 2024 The Authors. Published by Elsevier B.V. This is an open access article under the CC BY license (<http://creativecommons.org/licenses/by/4.0/>).

g. quantifying the spatial probability of exceeding national regulatory limits, and to outline As major sources and drivers.

1. Introduction

High Arsenic (As) concentration in groundwater is of large concern worldwide and affects a variety of environments and all types of aquifers: deep aquifers (Warner, 2001; Bošnjak et al., 2013; Khan et al., 2019) inland and coastal aquifers (Smedley and Kinniburgh, 2022). In coastal aquifer elevated ionic strength of groundwater and reducing conditions may often lead to high natural background levels of As, for example in the shallow coastal aquifer of Pearl river delta (Huang et al., 2018; Huang et al., 2023) in the Mekong delta and in the Po river delta (Erban et al., 2014) and along the Northern Adriatic Sea (Marconi et al., 2011; Greggio et al., 2020; Filippini et al., 2021).

As may naturally occur in groundwater under both reducing and oxidizing conditions. In strongly reducing conditions As mobilization occurs by a complex combination of redox reactions that involve reduction of the solid-phase As to As(III), desorption of As from Fe oxyhydroxides, reductive dissolution of these oxides and changes in Fe oxyhydroxides structure and surface properties in response to the establishment of reducing conditions (Smedley and Kinniburgh, 2022; Khan and Rai, 2023). Sulfide presence can also impact arsenic mobility under reducing conditions; if sulfide is present, arsenic and sulfide may precipitate, reducing arsenic mobility. The common As bearing minerals that can be natural sources of As are Arsenopyrite (FeAsS), Realgar (AsS), Enargite (CuAsS₄), and As₂S₃ (Bose and Sharma, 2002). Reduced arsenic-bearing minerals may experience oxidizing conditions when exposed to the atmosphere, whether through erosion, geothermal activities, or anthropogenic actions such as mining. This exposure leads to the release of As(III) and sulfate. The dissolution rate is highly influenced by the presence of oxygen and the rate of sulfide oxidation. Following release, arsenic (III) is reported to undergo partial or complete oxidation to As(V) by reactions mediated by bacteria (Wilkie and Herling, 1998). As occurrence is often related also to organic layers and humic substances in soils (Varsányi et al., 1991; Stuckey et al., 2015), and to dissolved organic carbon (DOC) in groundwater (Pi et al., 2015; Cui and Jing, 2019). In oxidizing environments, under conditions of high pH, As is present predominantly as As(V) in the form of arsenate AsO₄³⁻ and hydrogen arsenate HAsO₄²⁻ (Brookins, 2012). Metal oxides in the sediments (especially Fe and Mn oxyhydroxides) are thought to be the main source of dissolved As, due to desorption under basic conditions (Smedley and Kinniburgh, 2022).

As pollution due to anthropogenic causes, including mining activities, combustion of fossil fuels, use of arsenical pesticides, herbicides and crop desiccants, and additives to livestock food, is largely reported in the literature but tend to be localized rather than widespread (Williams, 2001; Li and Chen, 2005; Higgins et al., 2021).

As concentrations in the multilayer aquifers of the Padana Plain (Rotiroti et al., 2017) showed that shallow aquifers of some areas (i.e. Lombardy) are affected by natural As-pollution, while deep aquifers show evidence of As concentration increase because of drawdown of As-rich groundwater from overlying aquifers. In such environments, As release in groundwater is controlled by the simultaneous equilibrium between Fe-oxide and sulfate reductive dissolution, and FeS precipitation (Molinari et al., 2013; Rotiroti et al., 2015). In the Venetian plain, As concentration above 300 µg/l has been measured in shallow groundwater surrounding the Brenta River. Here, a lithological discontinuity (from coarse to silty sand) and the presence of thin layers of diffused sedimentary organic matter (SOM) along with anoxic conditions caused SOM degradation and enrichment of NH₄⁺ and As in groundwater (Carraro et al., 2013). Even in Lombardy and Emilia-Romagna regions the presence of peaty lenses is identified as the main driver of As release in groundwater (Rotiroti et al., 2014; Filippini et al.,

2021). In a study by Colombani et al. (2015) where high-resolution multi-level samplers were employed to monitor the coastal phreatic aquifer of Ferrara (Emilia Romagna region), As concentrations of up to 47 µg/l along with peaks of P, Fe²⁺, and HCO₃⁻ were found in reducing saline groundwater in contact with high SOM and pyrite sediments.

Since groundwater quality is driven by physical and chemical patterns determined by both geological factors and anthropogenic activities, the use of geostatistical methods could help to disentangle the spatial distribution and origin of dissolved contaminants. Nowadays, different geostatistical techniques are widely used to assess the spatial variations of groundwater quality: Kriging and Cokriging (Belkhiri et al., 2020; Farzaneh et al., 2022); integrated approach of multivariate statistical analysis and geostatistical methods (Huang et al., 2013; Cai et al., 2015; Chaudhry et al., 2019); integration of GIS and geostatistical techniques (Venkatraman et al., 2019); Monte Carlo-based and Sequential Simulations approaches (Remy et al., 2009; Schiavo, 2022; Schiavo et al., 2023). These stochastic methods are well-known and widely applied for estimating a spatially distributed variable to its simulation, hence entering the domain of probabilities. Recently, these have been applied for the understanding and quantification of natural As background levels in the Emilia-Romagna region (Molinari et al., 2019; Guadagnini et al., 2020), which is a portion of the domain here investigated.

Although geostatistical analysis has been effectively used to characterize and understand groundwater variables in space and time, its applicability is often limited by data availability and distribution. Geostatistical methods require enough data to adequately characterize spatial variability and in many cases data on groundwater quality may be limited, especially in terms of spatial coverage and depth. If the sampling density is insufficient, the heterogeneity at the local scale might not be adequately captured, affecting the reliability of results, and leading to large uncertainties.

The As contamination in the Padana Plain has been investigated for local case studies in the past (Carraro et al., 2013; Di Giuseppe et al., 2014; Natali and Bianchini, 2017), or at most for regional-scale analysis (Molinari et al., 2019; Guadagnini et al., 2020; Filippini et al., 2021). However, so far, a large-scale investigation considering the entire Padana Plain and including all available datasets is not present for Northern Italy. Moreover, the (even probabilistic) As contamination assessment should respect the integrity of the Padana Plain from a hydrogeological perspective, hence considering the whole area and local aquifer extensions. Indeed, a geographic partition of the Padana Plain might frame interconnected As contaminations as not spatially correlated, or depending on sediments with different origins, while a comprehensive statistical analysis of the entire Padana Plain allows a broad view of potential As contamination sources throughout the area.

This paper presents a large-scale geostatistical investigation of the As occurrence in the confined and phreatic aquifers of the Padana Plain to assess the spatial variability of concentration and quantify the probability of exceeding the WHO limit within different groundwater domains, disregarding the administrative limits. The 2018 groundwater databases of the Northern Italian ARPA (Piedmont, Lombardy, Veneto, Friuli-Venezia Giulia, and Emilia-Romagna) were used to retrieve As concentrations in groundwater and perform Monte Carlo (MC) simulations. Results of the stochastic modeling of large-scale As fields are then discussed with respect to hydrogeochemical information using scatter plots and Principal Component Analysis (PCA). Critical areas of As concentration have been identified, which can provide relevant information to water management authorities for future detailed studies.

2. Material and methods

2.1. Study area

The research area encompasses the major river basins of Northern Italy, and it is bounded by the Apennines in the South and South-West, by the Alps in the West, North, and North-East, and by the Adriatic Sea in the East (see it in Fig. 1 a, enclosed within the blue dotted polygon). In the western sector, which includes the Western Apennines, and Western and Central Alps, crystalline, metamorphic, and ophiolite complexes are the main geological features. The southern and eastern Alps, drained by northern Adriatic rivers, are mainly characterized by carbonate outcrops. The sediment transported by the Apennine rivers primarily originates from Cretaceous to Pliocene sedimentary successions, dominated by chaotic clays, turbidites (sandstone/marl alternations), and sandstones (Amorosi et al., 2002) (Fig. 1b).

The Padana Plain, drained by the Po River, occupies most of the study area (Fig. 1a) and can be subdivided into minor alluvial sectors, including the Venetian-Friulian Plain, the Lombardy-Piedmont Plain, and the Emilia-Romagna Plain. The Po Basin is filled with Plio-Quaternary sediments, reaching up to 8 km in thickness in the main depocenters south of the Po River, with a gradual thinning northward (Castaldini et al., 2019). The sedimentary infill exhibits a shallowing-upward trend, transitioning from deep-marine Pliocene deposits to shallow-marine and continental Quaternary deposits (Ori, 1993). The region is characterized by extensive alluvial fans, composed of Late Pleistocene fluvio-glacial deposits, and a cyclic change in fluvial-channel stacking pattern reflecting glacial-interglacial periods during the Middle-Late Pleistocene. Coastal plains exhibit vertically stacked deposits, alternating between coastal to marine (interglacial) and continental (glacial) sediments (Campo et al., 2020).

Due to the complex geological evolution of the study area and the cyclic alternation of vertically-stacked coarse- (fluvial to coastal) and fine- (alluvial to marine) grained strata, the hydrogeological setting is characterized by the presence of multi-layer aquifers with shallow phreatic aquifers and deeper, semi-confined and confined aquifers with variable thickness and hydraulic connectivity. Phreatic aquifers comprise coarse-grained sedimentary units, approximately 30 m thick, characterized by gravel and sand bodies; while fine-grained units made of silts and clays, with thickness ranging from about 5 to 50 m, act as main aquiclude and/or aquitards (Massari et al., 2004; Martinelli et al., 2018; De Luca et al., 2020; Fabbri and Piccinini, 2022). These unconfined shallow aquifers are generally discontinuous and poorly connected to underlying ones. Towards the coastline, due to the presence of continental alluvial deposits that overlay coarse-grained sedimentary units, the phreatic aquifers become locally semi-confined, resulting in reduced rates of recharge and discharge (Giambastiani et al., 2013).

At the margin of the Alpine and Apennine chains, alluvial fans are found and are characterized by generally high hydraulic conductivity (up to $1-10 \cdot 10^{-3}$ m/s for gravel and sand layers). These deposits represent the main direct recharge area of the entire hydrogeological system, including the deepest aquifers (Fontana et al., 2014). The transition from coarse-grained to finer-grained sediments in the distal regions of the alluvial plains leads to a decrease in hydraulic conductivities generally to $1-10 \cdot 10^{-5}$ m/s. Downwards in the Late Quaternary succession of the Padana Plain, multiple confined aquifers are then recognized within the entire hydrogeological system (Martinelli et al., 2018). Hydraulic gradients are highest near the Alpine and Apennine chains (8–4 ‰), decreasing towards the more distal low plains in the central-eastern Padana plain (0.2–1 ‰) (Martinelli et al., 2018; Giambastiani et al., 2013). This transition is accompanied by the emergence of lowland springs, known as “fontanili,” particularly in the Veneto-Friulan plain and along the left bank of the Po River. Groundwater flow generally moves towards the Po River, influenced by its drainage activity in the central-western sector, while in the east, the Po River is not hydraulically connected to groundwater.

The Po River valley has been the subject of several studies on sediment provenance aiming at defining the composition, geochemistry, and paleoenvironmental evolution of the area also providing insights into changes in the river system (Amorosi et al., 2002; Amorosi and Sammartino, 2007; Picone et al., 2008; Greggio et al., 2017; Natali and Bianchini, 2017; Bruno et al., 2021; Demurtas et al., 2022). Bulk-sediment geochemistry has been used to find proxies for sediment provenance and three compositional end-members, corresponding to the main geological domains, have been suggested: Dolomites (corresponding to Eastern Alps), Po (corresponding to Po River catchment), and Apennines (corresponding to the area where Apennine rivers reach the Adriatic Sea, Fig. 1b) (Picone et al., 2008; Greggio et al., 2017; Amorosi et al., 2022). The sediments of the Po River catchment are marked by elevated Cr and Ni concentrations (Amorosi et al., 2002; Amorosi and Sammartino, 2007). These high metal concentrations originate from the erosion of extensive ophiolite complexes present in the Western Alps and the northwestern Apennines. Conversely, sources from the Apennines exhibit lower Cr and Ni values (Amorosi et al., 2002), but display relatively higher CaO and Sr contents stemming from the Miocene Marnoso-arenaceous turbiditic Formation of the Romagna Apennines (Lancianese and Dinelli, 2015). Sediments from the Dolomites are identifiable by MgO as a tracer due to the prevalence of dolomite-rich rocks within their river catchments (Picone et al., 2008).

2.2. Groundwater database

In Italy, the Regional Environmental Protection Agencies (ARPA) are responsible for monitoring the quantity and quality of surface and groundwater bodies by European directives (Water Framework Directive; WFD, 2000) and international standards (WHO, 2017).

In this study, the 2018 database developed and reviewed by Orecchia et al. (2022) was employed< it consists of 3671 groundwater samples provided by the ARPAs of Lombardy, Piedmont, Veneto, Friuli-Venezia Giulia, and Emilia-Romagna through their OpenData portals. The database was integrated with information on sampling stations and the groundwater samples were grouped according to the type of aquifer (phreatic or confined) and the monitoring depth. More details about database design, data homogenization, and management are reported in Orecchia et al. (2022).

For the present work, the concentration of As ($\mu\text{g/l}$), along with the principal physical and chemical parameters, such as pH, temperature (T in $^{\circ}\text{C}$), electrical conductivity (EC in $\mu\text{S/cm}$), Cl^{-} and redox-sensitive species, i.e. NO_3^{-} , NH_4^{+} (mg/l), Mn and Fe ($\mu\text{g/l}$), were used. Sampling frequencies are defined by each region and variable, with at least 2 samples per year, one in the warm season (spring-summer) and one in the cold season (autumn-winter). It is also important to highlight that, given the challenge of distinguishing between confined and semi-confined aquifers in the complex multilayer hydrogeological setting of the Padana Plain (Fig. 1a), data from both confined and semi-confined aquifers were considered and analyzed together for the geostatistical assessment. Among the 3671 samples, 2243 belong to the phreatic aquifers and 1428 to confined aquifers. For 3412 samples it was possible to calculate the ion balance for accuracy control: 2895 samples had a cation-anion balance between -5% to $+5\%$, while 3151 samples had an ion balance within the range of -10% to $+10\%$, accounting for 85% and 92% of the entire database, respectively. All concentration values below the detection limit ($<\text{D.L.}$) were replaced with half of the identified detection limit, according to the methods proposed by Helsel et al. (2020) and expressly described for this database in Orecchia et al. (2022). For the statistical analysis, if more than one As concentration is available at a well's location (for the phreatic or the confined aquifers), the average value among available ones has been considered. A statistical summary of the groundwater sample composition is reported in Supplementary Information (Table S1).

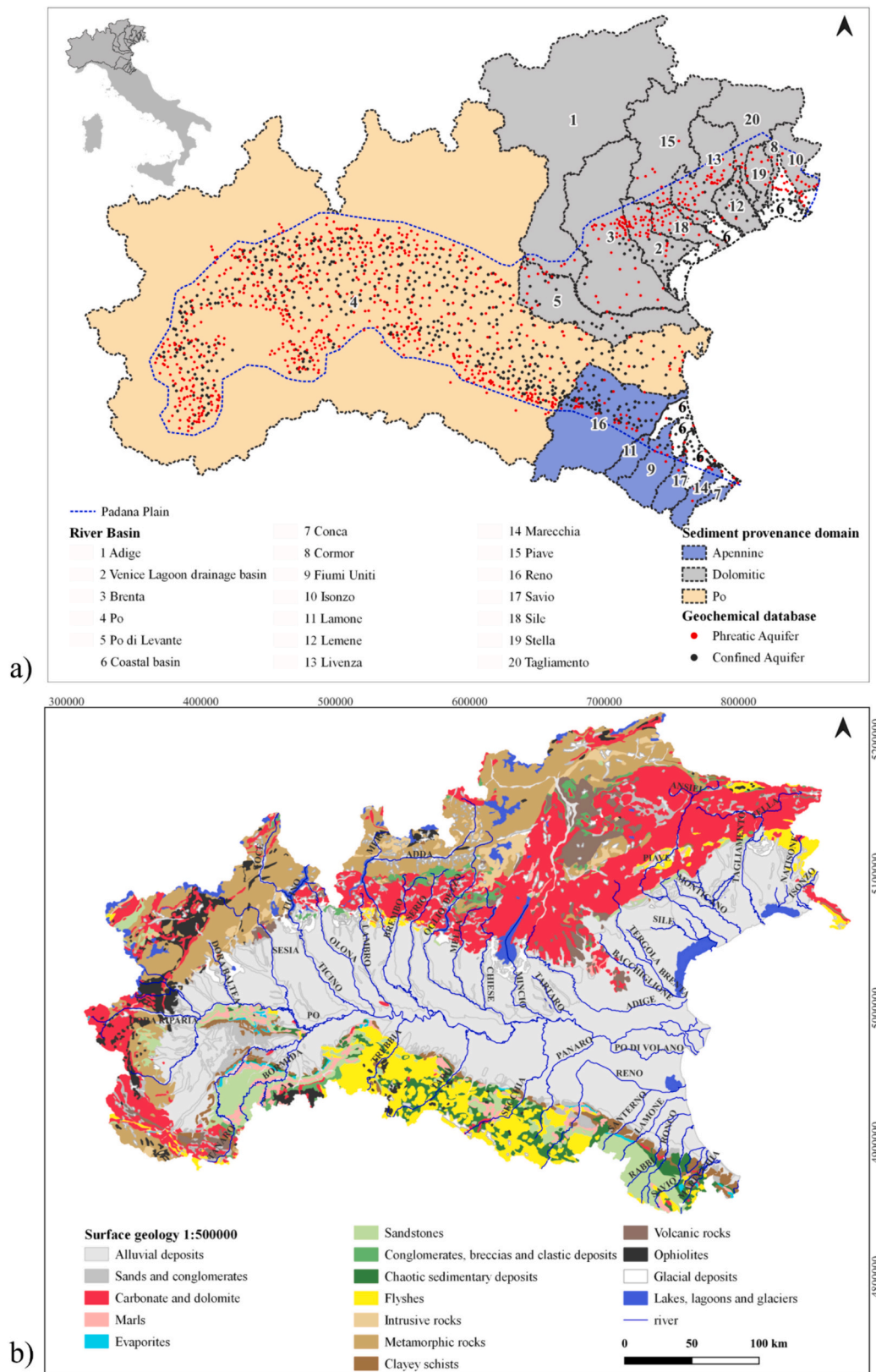


Fig. 1. a) Extension of the study domain and available geochemical database (boreholes in phreatic and confined aquifers in red and black colors, respectively); Padana Plain domain, river catchments and sediment provenance domain are also shown; b) lithology (from Geological Map of Italy, 1:500,000; modified from Orecchia et al., 2022).

2.3. Geostatistical approach

The domain is characterized by partitioning the Padana Plain in its hydrological basins and is discretized in squared cells of 1 km side, for a total amount of 1.4×10^5 cells. Each i -th cell barycenter is identified by its geographical coordinates $\mathbf{x}_i = (x_i, y_i)$. Depth-averaged As concentrations were identified by each borehole coordinates $\mathbf{x}_N = (x_N, y_N)$. A variogram analysis is employed to study the spatial correlation of measured As concentrations throughout the domain, splitting the analysis upon As measurements related to the phreatic and confined aquifers. The aim is to measure the spatial correlation between measured As concentration in each aquifer body, hence simulating many equiprobable concentration scenarios and embedding each i -th domain site with as many possible As simulated concentrations within a MC framework (Section 3.1), while honoring data where these are available. The domain is regarded as bidimensional since the spatial extension of aquifers (about 500 km \times 300 km) is several orders of magnitudes larger than boreholes' maximum local depths (200–300 m; Orecchia et al., 2022). The spatially distributed As stochastic fields represent a depth-averaged simulation of local concentrations across the local aquifer thickness.

Once this step is accomplished, a proper variogram model is calibrated for data within both the phreatic and confined domains. For each domain, a best-fitting exponential function is determined to be used in the simulation of stochastic fields of the variable of interest. No preferential variogram directions, hence anisotropies, emerged for data spatial correlation, hence an isotropic omnidirectional (exponential) variogram model is employed to interpret the dataset spatial correlation:

$$\gamma(h) = \sigma_N^2 \exp(1 - 3h/a) \quad (1)$$

where $h = \|\mathbf{x} - \mathbf{x}'\|$ is the separation distance between vector locations \mathbf{x} and \mathbf{x}' for each N -th borehole of the dataset; σ_N^2 and a are model parameters, corresponding to the variogram sill (i.e., experimental variance) and range, respectively. Measurements of As concentrations associated with phreatic aquifers are modeled upon an exponential variogram with a correlation scale of 155 km of the normal scored variogram, estimated via a Maximum Likelihood procedure (details not shown); while for confined aquifers the variogram is detrended upon a linear best-fitting function. The correlation of residuals retained a correlation scale of 160 km of the normal scored variogram, appraised through a Maximum Likelihood estimation procedure. Stochastic (conditional) depth-averaged As fields rely upon the dataset described in Section 2.2.

2.4. Stochastic modeling of large-scale arsenic fields

A well-known and widely applied geostatistical methodology, Sequential Gaussian Simulations (Remy et al., 2009) was employed to sequentially simulated spatially distributed As concentration fields, hence, to work within a MC framework (e.g. Schiavo, 2022; Schiavo et al., 2023). This approach enables to move from the discrete characterization of local As concentrations to the stochastic one, spatially distributed at the chosen grid scale. Therefore, each cell barycenter is associated with as many possible (equiprobable) simulated values as the number of performed simulations within the MC ensemble, i.e. a local concentration value $c_i = c(\mathbf{x}_i)$ for each simulation run. Then, the results are collected within the MC framework to be treated as a simulation ensemble.

The stochastic As concentration fields have been employed for three purposes: (i) considering them one by one as random fields, with locally varying spatial patterns; (ii) thresholding each random field upon the Italian national regulatory limit of 10 $\mu\text{g}/\text{l}$ for As in groundwater, which follows the WHO drinking water limits (WHO, 2017), hence embedding data location upon a logical variable (0 or 1) for exceeding the prescribed threshold or not; (iii) considering the local mean across

simulations ensemble (local MC-averaged values) to have the most probable one at each domain location. These operations move the analysis towards the domain of probabilities. This can be explained by introducing an indicator variable as follows:

$$I_r(\mathbf{x}_i) = \begin{cases} 1 & \text{if } c_r(\mathbf{x}_i) \geq thr \\ 0 & \text{if } c_r(\mathbf{x}_i) < thr \end{cases} \quad \text{with } r = 1, R \quad (2)$$

$r = 1, R$ being each MC simulation, $c_r(\mathbf{x}_i)$ the local simulated As concentration value at the i -th cell of the r -th realization, and $I_r(\mathbf{x}_i)$ is the value of $I(\mathbf{x}_i)$ in realization r of the ensemble. Then, $\chi(\mathbf{x}_i)$ was computed as:

$$\chi(\mathbf{x}_i) = \frac{1}{R} \sum_{r=1}^R I_r(\mathbf{x}_i) = \frac{q}{R} \quad (3)$$

q (an integer between 1 and R) being the number of MC simulations where the indicator is equal to one at the i -th location. Therefore, the indicator $I(\mathbf{x}_i)$ is a random variable that follows a Bernoulli distribution with probability $\chi(\mathbf{x}_i)$ given by $\Pr[I(\mathbf{x}_i) = 1] = \chi(\mathbf{x}_i)$. Such a probabilistic approach (Schiavo, 2022) enables stochastically assessing local probabilities of As concentrations and areas most likely to be contaminated.

Besides the probabilistic approach, scatterplots of As concentrations vs physical-chemical parameters allowed to identify the most likely geochemical processes taking place in the phreatic and confined aquifers. Moreover, the analysis considers major basins in Northern Italy as depositional environments, aiming to correlate the type of debris and the origin of sediments with local simulated MC concentrations. Some statistical considerations about simulated MC concentration density functions and their statistical moments in the phreatic and confined aquifers return a full assessment of As distribution and behavior in each groundwater body. Using PAST Software, in the end, "PCA" the Principal Component Analysis of log normal transformed raw data has been used to compute principal components (PCs) using the varimax rotation option. Of the original 35 parameters in the database, Zn, V, Hg, Sb, Se, Cu, Cr(VI) and hardness were excluded since the first 5 were mostly below detection limits and the latter being the sum of dissolved Ca and Mg.

3. Results

3.1. Stochastic and MC-averaged As concentration fields

The stochastic modeling permits to retrieve of many scenarios of As contamination within the Padana Plain; for each MC simulation, a different spatially distributed simulated As field is achieved (see Supplementary Information Section for further details). Since the MC-ensemble of equiprobable (stochastic) As fields is supposed to be a Gaussian distribution of simulated As values in each domain cell, according to the well-acknowledged SGSIM procedure, the local mean across all simulated values is the most probable value in a certain location. Hence, the mean across all MC simulations returns the most probable contamination scenario throughout the whole domain. The MC-averaged local value at each domain cell represents the most probable value simulated for phreatic and confined aquifers (Fig. 3).

Fig. 2 displays the MC-averaged As fields obtained for the phreatic (panel a) and confined (panel b) aquifers. Small areas exceeding 20 $\mu\text{g}/\text{l}$ are evident in the central region along the Po River in both the phreatic and confined aquifers. Additionally, concentrations above 20 $\mu\text{g}/\text{l}$ are found along the southern coast. Most concentrations ranging between 10 and 20 $\mu\text{g}/\text{l}$ are concentrated within the current Po delta (Fig. 2a) and around the higher concentrations in the phreatic aquifer. This distribution extends southwards in the confined aquifer (Fig. 2b).

As contamination spreads seaward for phreatic aquifers, being prevalent in the deltaic environment of the Venice Lagoon, while significant As concentrations are encountered in the medium reach of the Po River. In confined aquifers, the contamination follows the Po River,

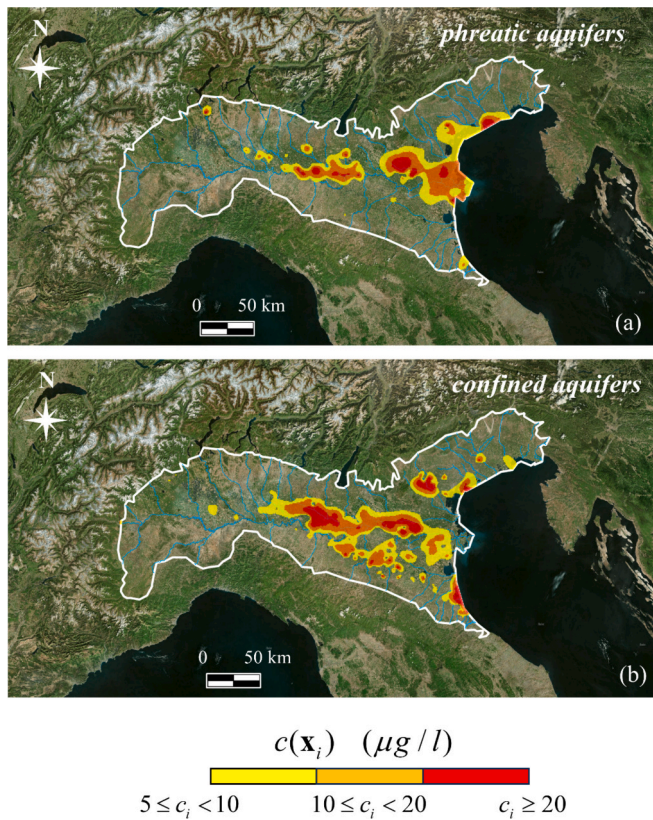


Fig. 2. MC-averaged As fields obtained for phreatic (panel a) and confined (panel b) aquifers as most probable contamination scenarios.

with two belts of elevated As concentrations in the center of the study area. For confined aquifers, a reduced continuity is present into the actual Po delta respect to phreatic aquifers, but other areas with higher As concentrations appear in the southern coastal portion (Fig. 2b). Nevertheless, the connectivity of high As concentrations within the confined aquifers in the medium and lower Po River path seems higher than in the phreatic ones. In general, high As simulated concentrations in confined aquifers are located farther to the outlet of surface water bodies than those simulated for phreatic aquifers.

The ratio of the area within the Padana Plain where the MC simulations returned As values above the regulatory limit of 10 µg/l was 13 % of samples from the confined aquifers and was 5 % from the phreatic aquifers. On average, the total area ratio embedded with over-threshold As values in about 3 % and 6 % in the phreatic and confined aquifers, respectively, with maximum possible area ratios of 12.8 % and 9.9 % (see Supplementary Information Fig. S2).

3.2. Statistics of Monte Carlo simulated fields

Fig. 3 shows statistics of simulated fields: panels (a) and (b) depict the empirical probability distributions of As concentrations in phreatic and confined aquifers, respectively. The simulated concentrations of confined aquifers are less prone to simulate negligible (close to zero) values, while being prone to simulate generally higher values, according to starting data (Fig. 3b). Fig. 3c shows that simulated concentrations in phreatic aquifers are less skewed than those in the confined ones. These statements are proved by investigating the first statistical moments of empirical distributions of phreatic and confined aquifers simulated concentrations. The higher mean skewness (Fig. 3e), hence the tendency to generate higher concentrations, is verified for confined aquifers, the variation on the mean of MC simulations is offered by the coefficient of variation, i.e. $c_v = \sigma_i / \mu_i$ μ_i being the data mean (µg/l) and variance σ_i (µg/l), respectively. Simulated concentrations in phreatic aquifers span over a wider range of values (Fig. 3d), thereby increasing the probability of various locations being characterized by either very low or high

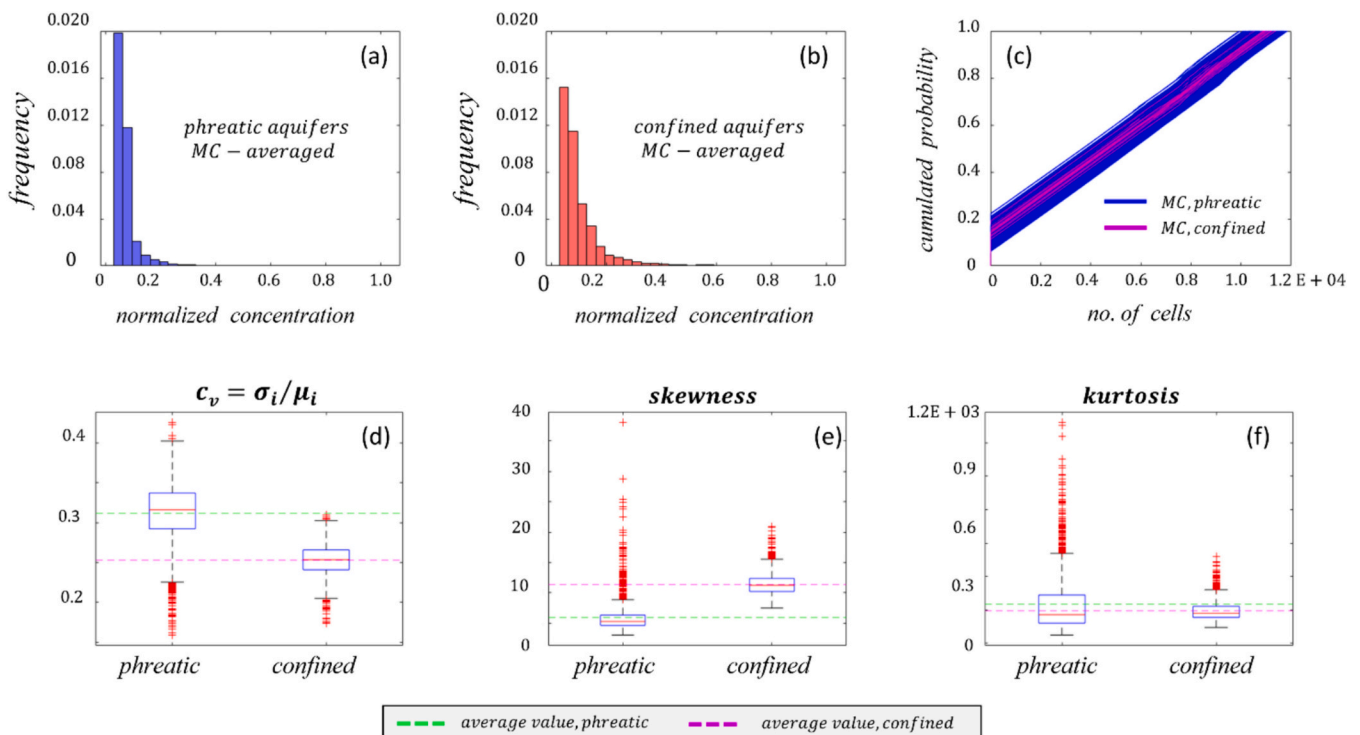
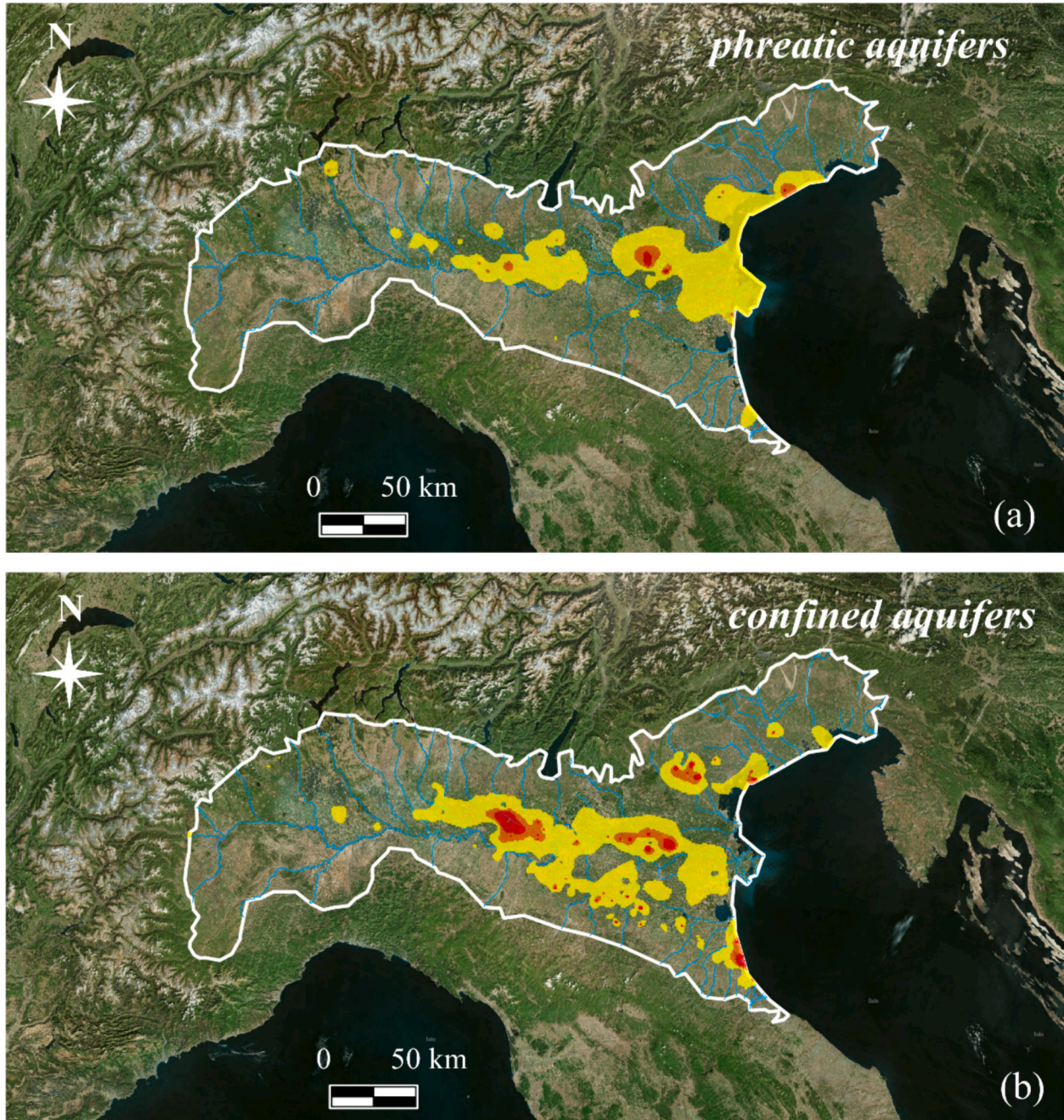


Fig. 3. Statistics of MC As fields for phreatic (a) and confined (b) aquifers. Cumulated MC probability functions (c) and statistical moments appraisal (panels d, e, and f) are also shown.

values compared to simulations based on confined aquifers data. A closer behavior to the normal distribution is expressed through kurtosis (Fig. 3f) for concentrations encompassing locations in the phreatic aquifers. This is attributed to slightly higher (median) values than those observed for confined aquifers, although the presence of several outliers is noted.

3.3. Probabilistic approach to arsenic spatially-distributed contamination

The multiple MC scenarios of possible As contaminations permits to assess the likelihood of a domain's locations exceeding the regulatory As limit (10 µg/l) in phreatic (Fig. 4a) and confined (Fig. 4b) aquifers. In phreatic aquifer, as in the case of MC-averaged concentration values (Fig. S2), the areas with the highest likelihood of exceeding the



$$\Pr [c(\mathbf{x}_i) \geq 10]$$



$$0.25 \leq \Pr < 0.50$$

$$0.50 \leq \Pr < 0.75$$

$$0.75 \leq \Pr < 1.00$$

Fig. 4. MC-averaged As probability fields obtained for phreatic (panel a) and confined (panel b) aquifers.

regulatory limit are in the proximity of the Venice lagoon and of the Adriatic Sea, which is the outlet of major rivers of the area (Fig. 4a), while for confined aquifers (Fig. 4b) they are concentrated in the medium-reach of the Po River and in the southern Padana Plain.

3.4. Spatial contamination across provinces and major river basins

Fig. 5 shows simulated concentrations and limit-exceeding probabilities across the major river basins in the Padana Plain, which are listed in Fig. 1b.

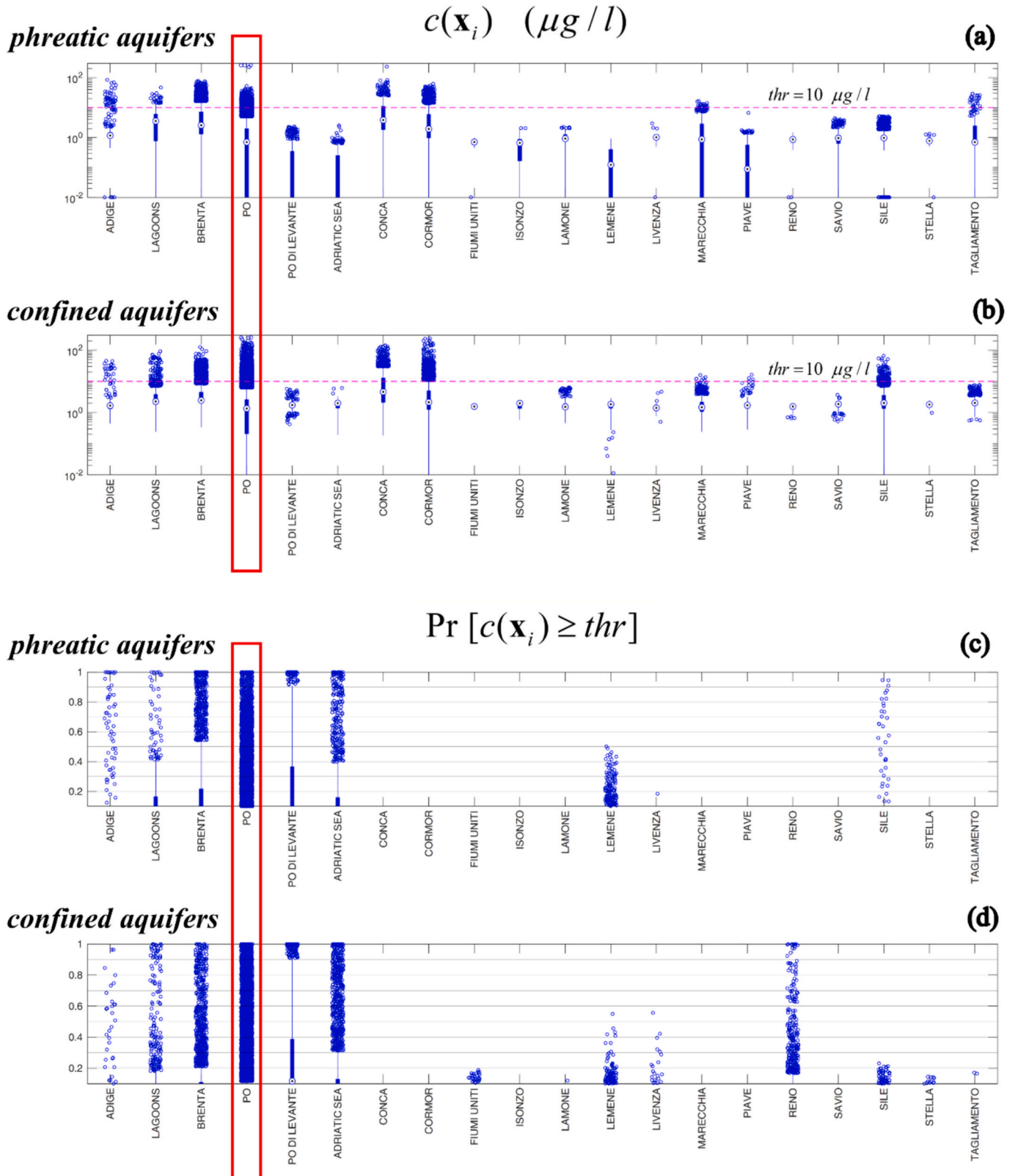


Fig. 5. Highly contaminated areas (a and b), and highly probable areas (c and d) characterized by limit-exceeding As contamination.

The spatial domain encompasses only the alluvial plain sector where the groundwater wells are installed, and groundwater samples are collected (Fig. 1a). The Po River basin is the widest and most contaminated basin in both phreatic and confined aquifers. However, very high concentrations and the corresponding limit-exceeding probabilities are identified even in the Brenta and Sile basins (Veneto Region). Similarly, elevated concentrations are found in the Friuli Venezia Giulia plain, particularly in smaller river basins such as Conca and Cormor (Fig. 5a and b). Nevertheless, it must be underlined the importance of further investigating the Padana Plain because of the numerosity of local limit-exceeding probability outliers and its role in driving the surficial water in Northern Italy.

Fig. 6 depicts high contamination values and probability along the Po River, with the positions of the major cities in the Po floodplain. This choice goes beyond the exemplary purpose since the Po River is the largest surface water body in Italy and its function as a drinking water source is fundamental for most of the human-related (both agricultural and industrial) activities in Northern Italy. Fig. 6a and b illustrate the profile of the As concentrations in phreatic and confined aquifers, while Fig. 6c and d show the probability to find As concentrations higher than 10 µg/l. The highest As concentrations are found in the Po riparian area between the cities of Piacenza and Ferrara for both the phreatic and confined aquifer systems. The highest probability of limit-exceeding As concentrations are simulated downstream the city of Piacenza, with peaks of about 0.75 and 0.60 for the phreatic and confined aquifers, respectively. In general, the probability of exceeding the regulatory limit along the Po River is lower for concentrations simulated within the confined aquifer than in the phreatic one.

3.5. Sediment provenance domain

Several studies in the past have identified three main geological domains in the study area that significantly influence sedimentary deposition: Po, Apennine and Dolomitic (Fig. 1a). Each domain affects the transported sediment by rivers and the resulting depositions (Greggio et al., 2017; Amorosi et al., 2002; Amorosi and Sammartino, 2007; Natali and Bianchini, 2017; Picone et al., 2008). This classification enables the identification of trends and provides a general accepted framework to individuate different geogenic sources for As concentration in groundwater.

Considering geochemical data and wells' locations, As occurrence in groundwater was investigated about the origin of local sediments according to previous studies (Greggio et al., 2017; Amorosi et al., 2002; Amorosi and Sammartino, 2007). In phreatic aquifers, most of the over-threshold As concentrations are measured where sediments have a Dolomitic or Po origin, while no concentrations higher than 10 µg/l are measured in sediments of Apennine origin (see Supplementary Information Fig. S3). In the confined aquifers most of the high As values are in correspondence of Dolomitic sediments, although several outlying ones are associated with the other types.

3.6. Groundwater geochemistry and PCA

Figs. 7 and 8 show the scatterplots of As versus main parameters and redox-sensitive species in both the phreatic and confined aquifers. Acidic environments are not a major driver of As release in solution, given that As has a normal distribution around circumneutral pH values (7.2–7.6). This is probably due to the presence of buffers like carbonates as previously reported (Rotiroti et al., 2014; Colombani et al., 2015; Orecchia et al., 2022). The release of As is also not linked to elevated temperatures since 75 % of samples have temperatures between 12.5 and 16.5 °C in the phreatic aquifer and between 13.5 and 16.5 °C in the confined aquifer. Besides, the outliers exhibiting low (<10 °C) and high (>20 °C) temperatures may be simply biased measurements due to cold or hot atmospheric conditions during sampling, as already demonstrated in this area (Colombani et al., 2016). Even EC, which is directly related

to TDS and thus to the mineralization of the samples, is not clearly related to As in groundwater, as well as to a conservative environmental tracer as Cl⁻. On the contrary, NO₃⁻ exhibits a marked hyperbolic relationship with As, since the latter is released in solution at post-oxic conditions in both phreatic and confined aquifers. The As correlation with Mn, Fe, and NH₄⁺ is less evident in phreatic aquifers, while in confined samples As show more direct relation with Fe and NH₄⁺, and marginally with Mn.

Prior to PCA elaboration, the Kaiser-Meyer-Olkin measure (KMO) reveal an “excellent” value of 0.82 and 0.84, respectively for phreatic and confined, indicating a suitability of the dataset for PCA. The PCs in Table 1 illustrate the results for the phreatic and confined aquifer data, respectively. Here, the PC1 in phreatic aquifers shows an agreement among EC and correlated elements (Cl⁻, Na⁺, Ca²⁺, Mg²⁺), while the PC2 is confirming that As is correlated with Fe, NH₄⁺, P, PO₄³⁻ and Mn, under reducing conditions. A reasonable negative correlation is evident in PC2 among As and NO₃⁻ and SO₄²⁻. In confined aquifer positive correlation exist among EC and connected elements but also Fe, NH₄⁺, Mn and minorly As has positive loadings indicating anoxic conditions. Similarly to phreatic aquifer also in confined PC2 shows agreement among As and Depth, pH, Fe, and PO₄³⁻ all of them having negative loadings.

The strong correlation observed in both aquifers between As and Fe, NH₄⁺, PO₄³⁻ suggests a significant influence of aquifer layers enriched in organic matter on the distribution of As. This dependency testifies the existence of anoxic conditions, where organic matter mineralization processes occur. On the contrary, the inverse correlation between As and molecules such as NO₃⁻ and SO₄²⁻ suggests that the presence of As is unlikely under oxic conditions (Rotiroti et al., 2014).

4. Discussion

The results of this study stand as the first large-scale spatial assessment of As groundwater contamination in Northern Italy. The ability to come up with spatial As fields is not limited to the quantification of local (possible) contaminations but enters the probability domain due to the stochastic framework implemented. This approach enables to retrieve the probability of a certain As concentration occurrence at each location of the modeled domain, and to properly relate it with the local geological and hydrological settings. One of the limitations of this approach is embedded within the spatial simulation technique, which simulates stochastic values within measurements' range, and is not able to predict eventual exceeding values. However, since the goal is to provide a full-scale assessment as close to data as possible, this inconvenience seems marginal. The approach is flexible and just data-driven, hence no conceptual priors for any hydrogeological or geochemical models are added. In this case, the lack of subjectivity is an additional strength of the approach, which aims at not altering data. Of course, the spatial reconstructions are dependent on the variogram modeling since the interpretation of experimental variograms is needed to achieve a mathematical structure for their modeling; but this is driven by best-fitting procedure of data and the flowchart is kept as neutral as possible. A limitation of the present analysis is that stochastic As fields are bidimensional, in fact no information about the measurement depths has been employed. Nevertheless, the extension of the domain compared to its average thickness can be considered large enough that even a bidimensional appraisal can fully capture the type of contamination and its spatial patterns. In addition, the choice made of going for a Kriging procedure and not for a multivariable spatial estimation (e.g. cokriging procedures) is supported by the poor data-grounded correlation between As and the other auxiliary variables. Moreover, the latter ones are not available as spatially distributed fields, covering the whole investigation area, so cokriging procedures cannot be performed at a first-stage analysis. In fact, despite the rich dataset available, all the information gathered is embedding wells' locations, i.e. are discrete information sources. Therefore, it is not possible to employ auxiliary variables to

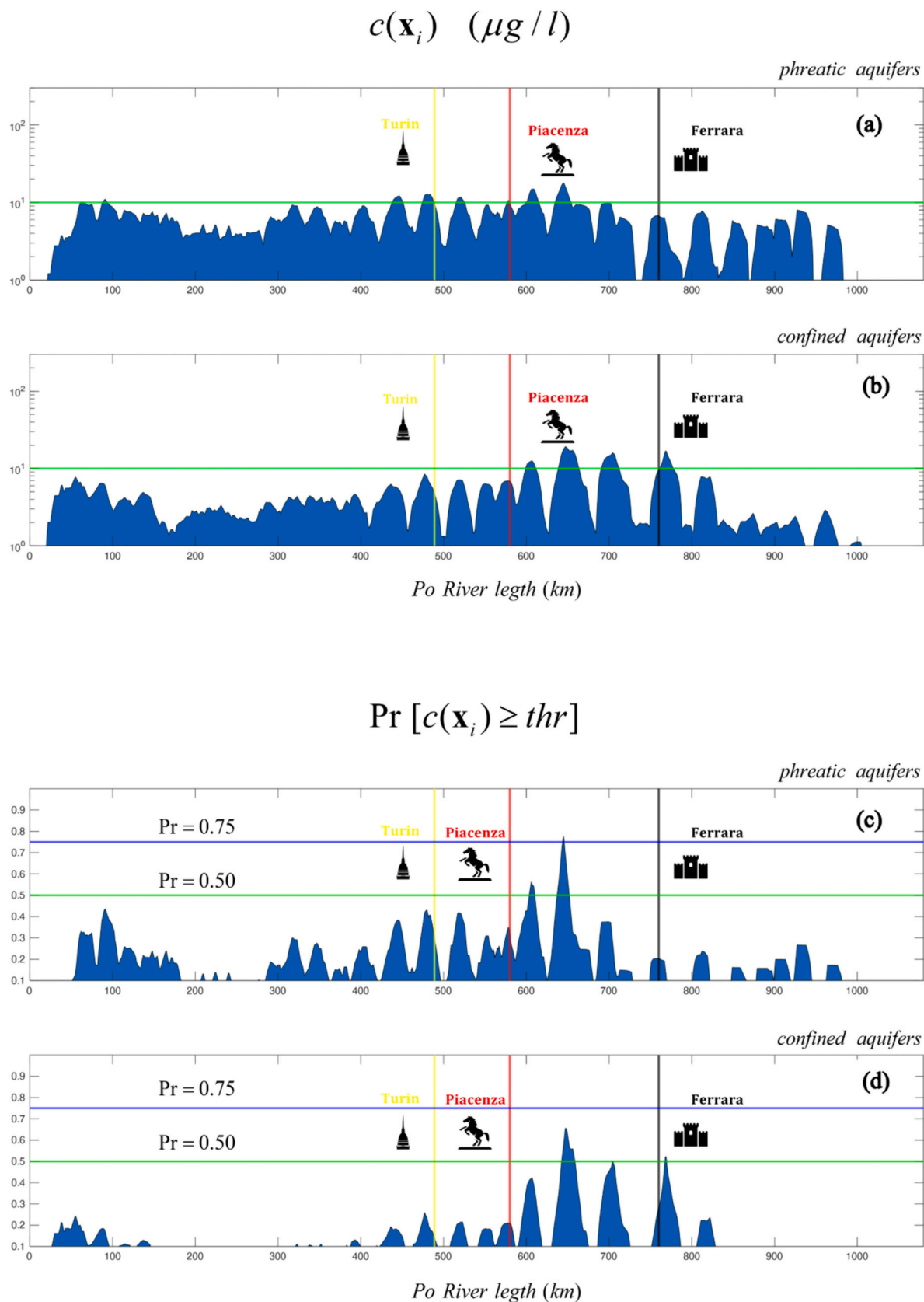


Fig. 6. Spatial extension of highly contaminated areas and highly probable areas characterized by limit-exceeding As contamination in the phreatic (a, c) and confined (b, d) aquifers.

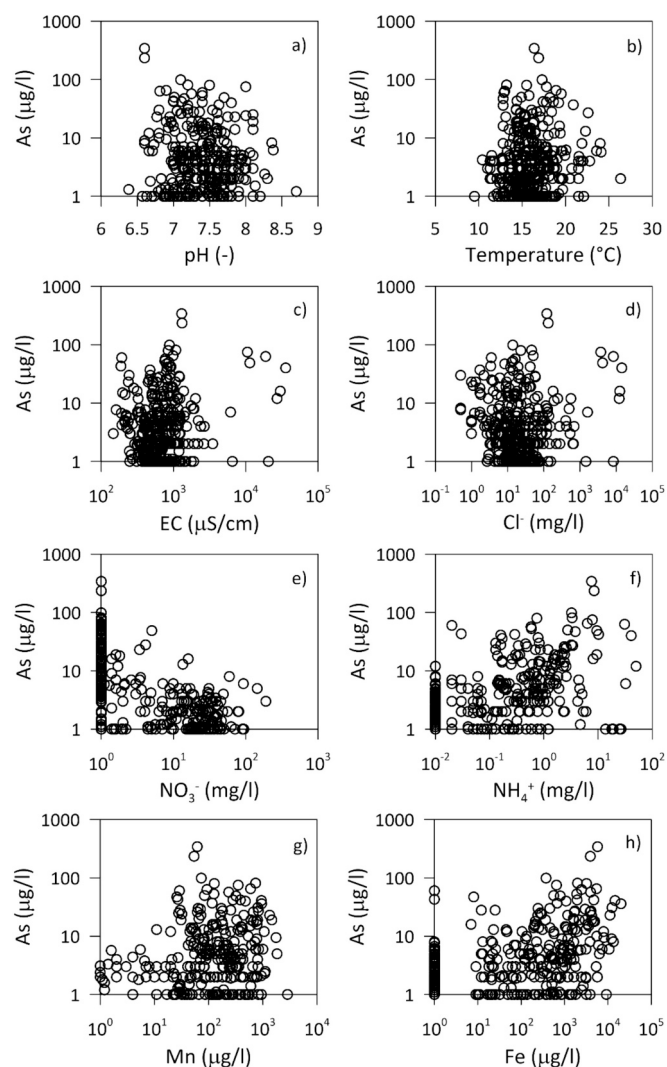


Fig. 7. Scatterplots showing the correlation between As concentrations (x-axis) and other auxiliary ones (y-axis) in confined aquifers. From panel a to h: As correlated with pH, Temperature ($^{\circ}\text{C}$), EC ($\mu\text{S}/\text{cm}$), Cl^{-} (mg/l), NO_3^{-} (mg/l), NH_4^{+} (mg/l), Mn ($\mu\text{g}/\text{l}$), and Fe ($\mu\text{g}/\text{l}$).

simulate spatially distributed As fields. Although many of the monitored data are involved in physical and chemical processes intimately related to As fate and transport, the modeling choices upon two points geostatistical methods can only pertain to As itself as the object a univariate geostatistical modeling. Even if in case of a cokriging relating As and another variable (see e.g. Deutsch and Journel, 1997), the spatially distributed (i.e. a map) representation of the latter one would not faithfully represent the real distribution of the variable itself, hence affecting the resulting co-kriged As field.

The most vulnerable areas are the Po, Adige, and Brenta river basins, with additional localized high As values observed in the small basins of Conca e Cormor within the Friuli-Venezia-Giulia region (Fig. 5). The Po River basin is the widest and most contaminated basin with the highest likelihood of exceeding the regulatory limit in the proximity of the Venice lagoon for the phreatic aquifers (Dalla Libera et al., 2015) and in the medium- and southern- reach of the Po River course for the confined aquifers (Figs. 4 and 6).

Based on hydrogeochemistry data, the presence of As in groundwater is related to Mn, Fe, and NH_4^{+} concentrations, especially in confined aquifers. This agrees with the literature results in this area that pointed out the release of As during reductive dissolution of Mn, Fe oxyhydroxides, and sedimentary-included organic matter mineralization

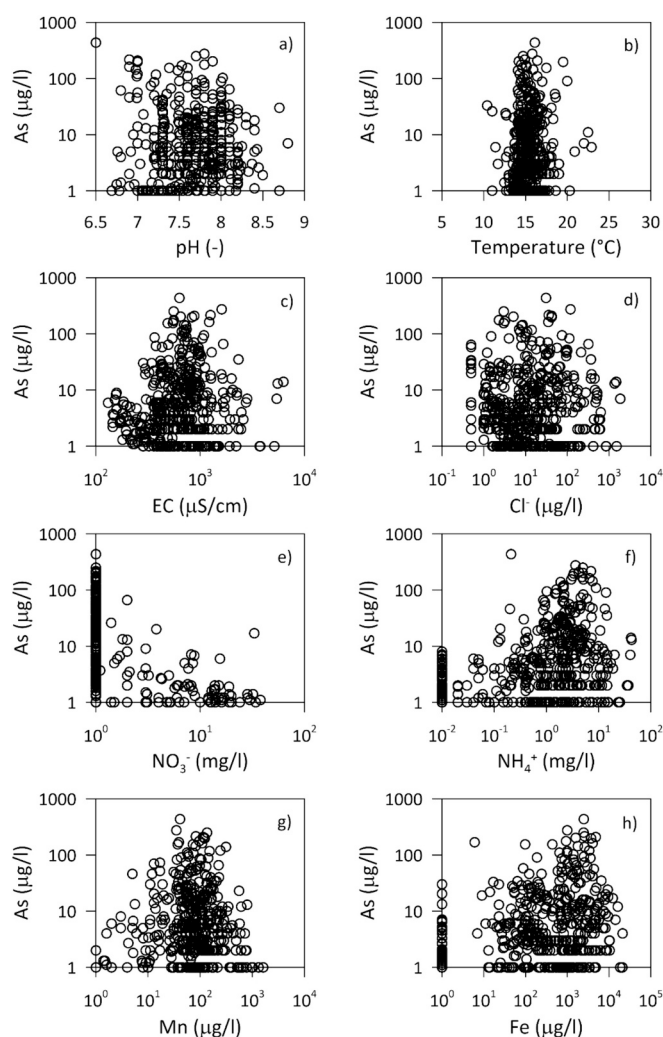


Fig. 8. Scatterplots showing the correlation between As concentrations (x-axis) and other auxiliary ones (y-axis) in confined aquifers. From panel a to h: As correlated with pH, Temperature ($^{\circ}\text{C}$), EC ($\mu\text{S}/\text{cm}$), Cl^{-} (mg/l), NO_3^{-} (mg/l), NH_4^{+} (mg/l), Mn ($\mu\text{g}/\text{l}$), and Fe ($\mu\text{g}/\text{l}$).

(peat layers) under anoxic conditions producing NH_4^{+} and P (Carraro et al., 2013; Molinari et al., 2013; Rotiroti et al., 2014; Colombani et al., 2015). These mechanisms are scarcely recognizable in the phreatic aquifer, but are more evident in the confined one, although the PCA confirmed the statistically relevant presence of As in Fe and Mn reducing conditions in both aquifer type. Despite a mixed oxic and reducing conditions that often develops in shallow aquifers and the length of the screens which is not adequate to capture such vertical gradients (Christensen et al., 2000; Coyte and Vengosh, 2020), the increase of Fe, and NH_4^{+} concentrations in groundwater due to the dissolution of oxides in reducing conditions and organic N mineralization correlates with an increase of As in the phreatic aquifer, as showed by the PCA results even if is not clearly visible in Fig. 7. In the confined aquifer, As concentrations peaks over distinct concentrations windows for Mn, Fe, and NH_4^{+} at around 0.1, 2.5, and 5 mg/l, respectively, indicating a control of Fe oxides reductive dissolution over As release with respect to other mechanisms. Even here, the PCA reveals an alignment of As loadings in concomitance with Fe and PO_4^{3-} possibly since many samples had As concentrations below detection limits or because of the monitoring wells screen length, as explained above.

Recent studies dealing with the paleoenvironmental evolution of the Padana Plain reveal that in the area between Mantova and Ferrara cities, during the last maximum marine ingressions (ca. 9 to 4 ky BP) a

Table 1

Principal component loadings (varimax rotated) for groundwater samples in phreatic and confined aquifers. Bold values are $>$ of 0.60, bold and italics values are $<$ -0.60 .

Parameters	Phreatic aquifers			Confined aquifers		
	PC1	PC2	PC3	PC1	PC2	PC3
As	0.20	0.69	0.03	0.21	-0.60	0.10
Depth	-0.40	-0.34	-0.20	-0.13	-0.41	-0.34
Temperature	0.24	0.24	0.19	0.17	-0.31	-0.03
pH	0.07	-0.06	-0.65	0.01	-0.54	0.10
Eh	-0.32	0.05	-0.28	-0.20	0.08	0.22
EC	0.90	-0.15	-0.26	0.88	0.32	0.09
HCO ₃ ⁻	0.74	-0.08	-0.54	0.89	0.12	0.15
Ca ²⁺	0.77	-0.27	-0.39	0.51	0.65	0.30
Cl ⁻	0.80	-0.16	0.26	0.72	0.43	-0.19
Fe	0.31	0.63	-0.11	0.65	-0.44	0.24
NH ₄ ⁺	0.25	0.49	-0.12	0.46	-0.30	-0.23
Mg ²⁺	0.76	-0.06	-0.29	0.80	0.29	0.06
NO ₃ ⁻	-0.21	-0.72	0.20	-0.45	0.68	-0.27
K ⁺	0.60	0.09	0.33	0.62	0.18	0.05
Na ⁺	0.83	-0.03	0.26	0.88	-0.12	-0.15
SO ₄ ²⁻	0.51	-0.49	0.17	-0.30	0.76	0.18
Ba	0.15	0.00	0.02	0.31	-0.29	-0.39
B	0.50	-0.14	0.38	0.49	-0.13	-0.56
Cd	0.15	0.09	0.05	0.01	0.01	0.07
Cr	-0.14	-0.06	0.13	-0.45	0.18	-0.31
F ⁻	0.53	-0.20	0.03	0.76	-0.01	-0.14
P	0.11	0.56	0.03	0.09	-0.28	0.39
Mn	0.34	0.42	0.00	0.43	0.02	0.26
Ni	0.22	0.03	0.46	0.01	0.33	-0.14
NO ₂ ⁻	0.19	0.11	0.24	-0.01	0.04	0.23
PO ₄ ³⁻	-0.10	0.57	0.03	-0.21	-0.41	0.40
Pb	-0.02	0.08	-0.03	-0.01	-0.06	-0.01
Eigenvalues	5.86	3.09	1.97	6.55	3.57	1.62
Explained variance (%)	21	11	7	24	13	6
Cumulative variance (%)	21	32	39	24	37	43

widespread peat deposit developed testifying a progressive flooding of the area during the last post-glacial sea level rise with the setting of deltaic environment (Bruno et al., 2021; Demurtas et al., 2022). These peat deposits could be subject to mineralization leading to As, Fe, Mn, and NH₄⁺ justifying the As concentration in Figs. 3a and 5a. In this area, even the Po River waters in base flow conditions witnessed a marked increase in As, with a peak of up to 18 µg/l respect to an average concentration of 12 µg/l (Marchina et al., 2015).

5. Conclusions

This study presents a robust and flexible geostatistical methodology to assess groundwater As probabilistic distribution in large basins like the Padana Plain, demonstrating its consistency with several types of information, including geological, geochemical, and hydrological data. The key contributions of the work are summarized as follows:

- i) It is the first comprehensive assessment of As contamination on a large scale, covering both phreatic and confined aquifers of the entire Padana Plain in Northern Italy. This strategic area, with its industrial, agricultural, and social significance, underscores the need for further investigations.
- ii) The geostatistical and statistical approach employed allowed for a thorough understanding of the spatial patterns of As contamination and to frame our results in a probabilistic framework, which is a novelty for this As contamination application. By adopting a probabilistic perspective, the local probability of exceeding regulatory limit was quantified, thus facilitating the identification of hazardous areas and their interconnections across the domain.

- iii) The most vulnerable areas are the Po, Adige, and Brenta river basins, with additional localized high As values observed in small basins within the Friuli-Venezia-Giulia region. The river basins with the highest concentration values are characterized by sediments with fluvio-glacial or dolomitic origins.
- iv) The release of As in groundwater in confined aquifers is linked to Mn, Fe, and NH₄⁺ concentrations driven by the reductive dissolution of Mn and Fe oxyhydroxides and the mineralization of organic matter under anoxic conditions. This phenomenon is less evident in phreatic aquifers, potentially due to mixed oxic and reducing conditions and insufficient monitoring sampling for capturing vertical gradients. In the confined aquifers, a major influence of Fe oxides reductive dissolution on As release compared to other mechanisms is evident, potentially tied to the mineralization of peat deposits formed during the last post-glacial sea level rise in the Padana Plain.

The study could improve the capability to simulate local As concentrations in large basins as well as those of auxiliary variables, identify hazardous areas, and assist local and national authorities in the sustainable and efficient management of groundwater resources.

Fundings

This research did not receive any specific grant from funding agencies in the public, commercial, or not-for-profit sectors.

CRedit authorship contribution statement

Massimiliano Schiavo: Writing – original draft, Visualization, Conceptualization, Data curation, Formal analysis, Investigation, Methodology, Software. **Beatrice M.S. Giambastiani:** Writing – review & editing, Visualization, Data curation. **Nicolas Greggio:** Data curation, Visualization, Writing – review & editing. **Nicolò Colombani:** Writing – review & editing, Visualization, Methodology, Conceptualization. **Micòl Mastrocicco:** Writing – review & editing, Validation, Conceptualization.

Declaration of competing interest

The authors declare that they have no known competing financial interests or personal relationships that could have appeared to influence the work reported in this paper.

Data availability

Data will be made available on request.

Appendix A. Supplementary data

Supplementary data to this article can be found online at <https://doi.org/10.1016/j.scitotenv.2024.172998>.

References

- Amorosi, A., Sammartino, I., 2007. Influence of sediment provenance on background values of potentially toxic metals from near-surface sediments of Po coastal plain (Italy). *Int. J. Earth Sci. (Geol. Rundsch)* 96, 389–396. <https://doi.org/10.1007/s00531-006-0104-8>.
- Amorosi, A., Centineo, M.C., Dinelli, E., Lucchini, F., Tateo, F., 2002. Geochemical and mineralogical variations as indicators of provenance changes in Late Quaternary deposits of SE Po Plain. *Sedim. Geol.* 151 (3–4), 273–292. [https://doi.org/10.1016/S0037-0738\(01\)00261-5](https://doi.org/10.1016/S0037-0738(01)00261-5).
- Amorosi, A., Sammartino, I., Dinelli, E., Campo, B., Guercia, T., Trincardi, F., Pellegrini, C., 2022. Provenance and sediment dispersal in the Po-Adriatic source-to-sink system unraveled by bulk-sediment geochemistry and its linkage to catchment geology. *Earth Sci. Rev.* 234, 104202 <https://doi.org/10.1016/j.earscirev.2022.104202>.

- Belkhir, L., Tiri, A., Mouni, L., 2020. Spatial distribution of the groundwater quality using kriging and Co-kriging interpolations. *Groundwater Sustain. Development* 11, 100473. <https://doi.org/10.1016/j.gsd.2020.100473>.
- Bose, P., Sharma, A., 2002. Role of iron in controlling speciation and mobilization of arsenic in subsurface environment. *Water Res.* 36 (19), 4916–4926. [https://doi.org/10.1016/S0043-1354\(02\)00203-8](https://doi.org/10.1016/S0043-1354(02)00203-8).
- Bošnjak, M.U., Casiot, C., Duić, Z., Fazinić, S., Halamić, J., Sipos, L., Santo, V., Dadić, Ž., 2013. Sediment characterization and its implications for arsenic mobilization in deep aquifers of eastern Croatia. *J. Geochem. Explor.* 126–127, 55–66. <https://doi.org/10.1016/j.gexplo.2012.12.017>.
- Brookins, D.G., 2012. *Eh-pH Diagrams for Geochemistry*. Springer-Verlag, Berlin, p. 176. <https://doi.org/10.1007/978-3-642-73093-1>.
- Bruno, L., Amorosi, A., Lugli, S., Sammartino, I., Fontana, D., 2021. Trunk river and tributary interactions recorded in the Pleistocene–Holocene stratigraphy of the Po Plain (northern Italy). *Sedimentology* 68 (6), 2918–2943. <https://doi.org/10.1111/sed.12880>.
- Cai, L., Xu, Z., Bao, P., He, M., Dou, L., Chen, L., Zhou, Y., Zhu, Y.-G., 2015. Multivariate and geostatistical analyses of the spatial distribution and source of arsenic and heavy metals in the agricultural soils in Shunde, Southeast China. *J. Geochem. Explor.* 148, 189–195. <https://doi.org/10.1016/j.gexplo.2014.09.010>.
- Campo, B., Bruno, L., Amorosi, A., 2020. Basin-scale stratigraphic correlation of late Pleistocene–Holocene (MIS 5e–MIS 1) strata across the rapidly subsiding Po Basin (northern Italy). *Quat. Sci. Rev.* 237, 106300. <https://doi.org/10.1016/j.quascirev.2020.106300>.
- Carraro, A., Fabbri, P., Giaretta, A., Peruzzo, L., Tateo, F., Teatini, P., 2013. Arsenic anomalies in shallow venetian plain (Northeast Italy) groundwater. *Environ. Earth Sci.* 70, 3067–3084. <https://doi.org/10.1007/s12665-013-2367-2>.
- Castaldini, D., Marchetti, M., Norini, G., Vandelli, V., Vélez, M.C.Z., 2019. Geomorphology of the Central Po plain. *Northern Italy. J. Maps* 15 (2), 780–787. <https://doi.org/10.1080/17445647.2019.1673222>.
- Chaudhry, A.K., Kumar, K., Alam, M.A., 2019. Groundwater contamination characterization using multivariate statistical analysis and geostatistical method. *Water Supply* 19 (8), 2309–2322. <https://doi.org/10.2166/ws.2019.111>.
- Christensen, T.H., Bjerg, P.L., Banwart, S.A., Jakobsen, R., Heron, G., Albrechtsen, H.J., 2000. Characterization of redox conditions in groundwater contaminant plumes. *J. Cont. Hydrol.* 45 (3–4), 165–241. [https://doi.org/10.1016/S0169-7722\(00\)00109-1](https://doi.org/10.1016/S0169-7722(00)00109-1).
- Colombani, N., Mastrocicco, M., Dinelli, E., 2015. Trace elements mobility in a saline coastal aquifer of the Po River lowland (Italy). *J. Geochem. Explor.* 159, 317–328. <https://doi.org/10.1016/j.gexplo.2015.10.009>.
- Colombani, N., Giambastiani, B.M.S., Mastrocicco, M., 2016. Use of shallow groundwater temperature profiles to infer climate and land use change: interpretation and measurement challenges. *Hydrol. Proc.* 30 (14), 2512–2524. <https://doi.org/10.1002/hyp.10805>.
- Coyte, R.M., Vengosh, A., 2020. Factors controlling the risks of co-occurrence of the redox-sensitive elements of arsenic, chromium, vanadium, and uranium in groundwater from the eastern United States. *Environ. Sci. Technol.* 54 (7), 4367–4375. <https://doi.org/10.1021/acs.est.9b06471>.
- Cui, J., Jing, C., 2019. A review of arsenic interfacial geochemistry in groundwater and the role of organic matter. *EcoTox. Environ. Safe.* 183, 109550. <https://doi.org/10.1016/j.ecoenv.2019.109550>.
- Dalla Libera, N., Fabbri, P., Piccinini, L., Pola, M., Mason, L., 2015. Natural arsenic in groundwater in the drainage basin to the Venice lagoon (Brenta plain, NE Italy): the organic matter's role. *Rend. Online Soc. Geol. It.* 41, 30–33. <https://doi.org/10.3301/ROL.2016.85>.
- De Luca, D.A., Lasagna, M., Debernardi, L., 2020. Hydrogeology of the Western Po Plain (Piedmont, NW Italy). *J. Maps* 16, 265–273. <https://doi.org/10.1080/17445647.2020.1738280>.
- Demurtas, L., Bruno, L., Lugli, S., Fontana, D., 2022. Evolution of the Po–Alpine River system during the last 45 kyr inferred from stratigraphic and compositional evidence (Ostiglia, northern Italy). *Geosciences* 12 (9), 342. <https://doi.org/10.3390/geosciences12090342>.
- Deutsch, C.V., Journel, A., 1997. *GSLIB: Geostatistical Software Library and User's Guide*. Oxford University Press, New York.
- Di Giuseppe, D., Faccini, B., Mastrocicco, M., Colombani, N., Coltorti, M., 2014. Reclamation influence and background geochemistry of neutral saline soils in the Po River Delta Plain (northern Italy). *Environ. Earth Sci.* 72, 2457–2473. <https://doi.org/10.1007/s12665-014-3154-4>.
- Erban, L.E., Gorelick, S.M., Fendorf, S., 2014. Arsenic in the multi-aquifer system of the Mekong Delta, Vietnam: analysis of large-scale spatial trends and controlling factors. *Environ. Sci. Technol.* 48 (11), 6081–6088. <https://doi.org/10.1021/es403932t>.
- Fabbri, P., Piccinini, L., 2022. Assessing transmissivity from specific capacity in an alluvial aquifer in the middle venetian plain (NE Italy). *Water Sci. Technol.* 67 (9), 2000–2008. <https://doi.org/10.2166/wst.2013.074>.
- Farzaneh, G., Khorasani, N., Ghodousi, J., Panahi, M., 2022. Application of geostatistical models to identify spatial distribution of groundwater quality parameters. *Environ. Sci. Pollut. R.* 29, 36512–36532. <https://doi.org/10.1007/s11356-022-18639-8>.
- Filippini, M., Zanotti, C., Bonomi, T., Sacchetti, V.G., Amorosi, A., Dinelli, E., Rotiroli, M., 2021. Deriving natural background levels of arsenic at the meso-scale using site-specific datasets: an unorthodox method. *Water* 13, 452. <https://doi.org/10.3390/w13040452>.
- Fontana, A., Mozzi, P., Marchetti, M., 2014. Alluvial fans and Megafans along the southern side of the Alps. *Sediment. Geol.* 301, 150–171. <https://doi.org/10.1016/j.sedgeo.2013.09.003>.
- Giambastiani, B.M.S., Colombani, N., Mastrocicco, M., Fidelibus, M.D., 2013. Characterization of the lowland coastal aquifer of Comacchio (Ferrara, Italy): hydrology, hydrochemistry and evolution of the system. *J. Hydrol.* 501, 35–44. <https://doi.org/10.1016/j.jhydrol.2013.07.037>.
- Greggio, N., Giambastiani, B.M.S., Campo, B., Dinelli, E., Amorosi, A., 2017. Sediment composition, provenance, and Holocene paleoenvironmental evolution of the southern Po River coastal plain (Italy). *Geol. J.* 53 (3), 914–928. <https://doi.org/10.1002/gj.2934>.
- Greggio, N., Giambastiani, B.M.S., Mollema, P., Laghi, M., Capo, D., Gabbianelli, G., Antonellini, M., Dinelli, E., 2020. Assessment of the main geochemical processes affecting surface water and groundwater in a low-lying coastal area: implications for water management. *Water* 12 (6), 1720. <https://doi.org/10.3390/w12061720>.
- Guadagnini, L., Menafoglio, A., Sanchez-Vila, X., Guadagnini, A., 2020. Probabilistic assessment of spatial heterogeneity of natural background concentrations in large-scale groundwater bodies through functional Geostatistics. *Sci. Total Environ.* 740 (2020), 140139. <https://doi.org/10.1016/j.scitotenv.2020.140139>.
- Helsel, D.R., Hirsch, R.M., Ryberg, K.R., Archfield, S.A., Gilroy, E.J., 2020. *Statistical methods in water resources*: U.S. Geological Survey Techniques and Methods, Book 4, chap. A3, 458. <https://doi.org/10.3133/tm4a3>.
- Higgins, M.A., Metcalf, M.J., Robbins, G.A., 2021. Nonpoint source arsenic contamination of soil and groundwater from legacy pesticides. *J. Environ. Qual.* 51, 66–77. <https://doi.org/10.1002/jeq2.20304>.
- Huang, G., Sun, J., Zhang, Y., Chen, Z., Liu, F., 2013. Impact of anthropogenic and natural processes on the evolution of groundwater chemistry in a rapidly urbanized coastal area, South China. *Sci. Tot. Environ.* 463, 209–221.
- Huang, G., Zhang, M., Liu, C., Li, L., Chen, Z., 2018. Heavy metal (loid) s and organic contaminants in groundwater in the Pearl River Delta that has undergone three decades of urbanization and industrialization: distributions, sources, and driving forces. *Sci. Tot. Environ.* 635, 913–925. <https://doi.org/10.1016/j.scitotenv.2018.04.210>.
- Huang, G., Song, J., Han, D., Liu, R., Liu, C., Hou, Q., 2023. Assessing natural background levels of geogenic contaminants in groundwater of an urbanized delta through removal of groundwaters impacted by anthropogenic inputs: new insights into driving factors. *Sci. Tot. Environ.* 857, 159527. <https://doi.org/10.1016/j.scitotenv.2022.159527>.
- Khan, M.U., Rai, N., 2023. Distribution, geochemical behavior, and risk assessment of arsenic in different floodplain aquifers of middle Gangetic basin, India. *Environ. Geochem. Health* 45 (5), 2099–2115. <https://doi.org/10.1007/s10653-022-01321-w>.
- Khan, M.R., Michael, H.A., Nath, B., Huhmann, B.L., Harvey, C.F., Mukherjee, A., Choudhury, I., Chakraborty, M., Ullah, M.S., Ahmed, K.M., Goodbred, S.L., Schlosser, P., Bostick, B.C., Mailloux, B.J., Ellis, T., van Geen, A., 2019. High-arsenic groundwater in the southwestern Bengal basin caused by a lithologically controlled deep flow system. *Geophys. Res. Lett.* 46, 13062–13071. <https://doi.org/10.1029/2019GL084767>.
- Lancianese, V., Dinelli, E., 2015. Different spatial methods in regional geochemical mapping at high density sampling: an application on stream sediment of Romagna Apennines, northern Italy. *J. Geochem. Explor.* 154, 143–155. <https://doi.org/10.1016/j.gexplo.2014.12.014>.
- Li, Y.X., Chen, T.B., 2005. Concentrations of additive arsenic in Beijing pig feeds and the residues in pig manure. *Resour. Conserv. Recy.* 45 (4), 356–367. <https://doi.org/10.1016/j.resconrec.2005.03.002>.
- Marchina, C., Bianchini, G., Natali, C., Pennisi, M., Colombani, N., Tassinari, R., Knoeller, K., 2015. The Po river water from the Alps to the Adriatic Sea (Italy): new insights from geochemical and isotopic ($\delta^{18}\text{O}$ - δD) data. *Environ. Sci. Pollut. Res.* 22, 5184–5203. <https://doi.org/10.1007/s11356-014-3750-6>.
- Marconi, V., Antonellini, M., Balugani, E., Dinelli, E., 2011. Hydrogeochemical characterization of small coastal wetlands and forests in the southern Po plain (northern Italy). *Ecohydrol* 4, 597–607. <https://doi.org/10.1002/eco.204>.
- Martinelli, G., Dadomo, A., De Luca, D.A., Mazzola, M., Lasagna, M., Pennisi, M., Pilla, G., Sacchi, E., Saccon, P., 2018. Nitrate sources, accumulation and reduction in groundwater from northern Italy: insights provided by a nitrate and boron isotopic database. *Appl. Geochem.* 91, 23–35. <https://doi.org/10.1016/j.apgeochem.2018.01.011>.
- Massari, F., Rio, D., Serandrei Barbero, R., Asioli, A., Capraro, L., Fornaciari, E., Vergerio, P.P., 2004. The environment of Venice area in the past two million years. *Palaeogeogr. Palaeoclimatol. Palaeoecol.* 202, 273–308. [https://doi.org/10.1016/S0031-0182\(03\)00640-0](https://doi.org/10.1016/S0031-0182(03)00640-0).
- Molinari, A., Guadagnini, L., Marcaccio, M., Straface, S., Sanchez-Vila, X., Guadagnini, A., 2013. Arsenic release from deep natural solid matrices under experimentally controlled redox conditions. *Sci. Tot. Environ.* 444, 231–240. <https://doi.org/10.1016/j.scitotenv.2012.11.093>.
- Molinari, A., Guadagnini, L., Marcaccio, M., Guadagnini, A., 2019. Geostatistical multimodel approach for the assessment of the spatial distribution of natural background concentrations in large-scale groundwater bodies. *Water Res.* 149, 522–532. <https://doi.org/10.1016/j.watres.2018.09.049>.
- Natali, C., Bianchini, G., 2017. Geochemical proxies of sediment provenance in alluvial plains with interfering fluvial systems: a study case from NE Italy. *Catena* 157, 67–74. <https://doi.org/10.1016/j.catena.2017.05.018>.
- Orecchia, C., Giambastiani, B.M.S., Greggio, N., Campo, B., Dinelli, E., 2022. Geochemical characterization of groundwater in the confined and unconfined aquifers of the northern Italy. *Appl. Sci.* 12 (15), 7944. <https://doi.org/10.3390/app12157944>.
- Ori, G.G., 1993. Continental depositional Systems of the Quaternary of the Po Plain (northern Italy). *Sedim. Geol.* 83, 1–14. [https://doi.org/10.1016/S0037-0738\(10\)80001-6](https://doi.org/10.1016/S0037-0738(10)80001-6).

- Pi, K., Wang, Y., Xie, X., Huang, S., Yu, Q., Yu, M., 2015. Geochemical effects of dissolved organic matter biodegradation on arsenic transport in groundwater systems. *J. Geochem. Explor.* 149, 8–21. <https://doi.org/10.1016/j.gexplo.2014.11.005>.
- Picone, S., Alvisi, F., Dinelli, E., Morigi, C., Negri, A., Ravaioli, M., Vaccaro, C., 2008. New insights on late quaternary paleo-geographic setting in the northern Adriatic Sea (Italy). *J. Quat. Sci.* 23 (5), 489–501. <https://doi.org/10.1002/jqs.1152>.
- Remy, N., Boucher, A., Wu, J., 2009. *Applied Geostatistics with SGeMS: A User's Guide*. Cambridge University Press. <https://doi.org/10.1017/CBO9781139150019>.
- Rotiroli, M., Sacchi, E., Fumagalli, L., Bonomi, T., 2014. Origin of arsenic in groundwater from the multilayer aquifer in Cremona (northern Italy). *Environ. Sci. Technol.* 48 (48), 5395–5403. <https://doi.org/10.1021/es405805v>.
- Rotiroli, M., Jakobsen, R., Fumagalli, L., Bonomi, T., 2015. Arsenic release and attenuation in a multilayer aquifer in the Po plain (northern Italy): reactive transport modeling. *Appl. Geochem.* 63, 599–609. <https://doi.org/10.1016/j.apgeochem.2015.07.001>.
- Rotiroli, M., McArthur, J., Fumagalli, L., Stefacia, G.A., Sacchi, E., Bonomi, T., 2017. Pollutant sources in an arsenic-affected multilayer aquifer in the Po plain of Italy: implications for drinking-water supply. *Sci. Tot. Environ.* 578, 502–512. <https://doi.org/10.1016/j.scitotenv.2016.10.215>.
- Schiavo, M., 2022. Probabilistic delineation of subsurface pathways in alluvial aquifers under geological uncertainty. *J. Hydrol.* 615, 128674 <https://doi.org/10.1016/j.jhydrol.2022.128674>.
- Schiavo, M., Colombani, N., Mastrocicco, M., 2023. Modeling stochastic saline groundwater occurrence in coastal aquifers. *Water Res.* 235, 119885 <https://doi.org/10.1016/j.watres.2023.119885>.
- Smedley, P.L., Kinniburgh, D.G., 2002. A review of the source, behaviour and distribution of arsenic in natural waters. *Appl. Geochem.* 17 (5), 517–568. [https://doi.org/10.1016/S0883-2927\(02\)00018-5](https://doi.org/10.1016/S0883-2927(02)00018-5).
- Stuckey, J.W., Schaefer, M.V., Kocar, B.D., Dittmar, J., Lezama Pacheco, J., Benner, S.G., Fendorf, S., 2015. Peat formation concentrates arsenic within sediment deposits of the Mekong Delta. *Geochim. Cosmochim. Acta* 149, 90–205. <https://doi.org/10.1016/j.gca.2014.10.021>.
- Varsányi, I., Fodré, Z., Bartha, A., 1991. Arsenic in drinking water and mortality in the southern Great Plain, Hungary. *Environ. Geochem. Health* 13, 14–22. <https://doi.org/10.1007/BF01783491>.
- Venkatramanan, S., Viswanathan Prasanna, M., Chung, S.Y., 2019. *GIS and Geostatistical Techniques for Groundwater Science*. Elsevier, p. 371. <https://doi.org/10.1016/C2017-0-02667-8>.
- Warner, K.L., 2001. Arsenic in glacial drift aquifers and the implication for drinking water - lower Illinois River basin. *Ground Water* 39 (3), 433–442. <https://doi.org/10.1111/j.1745-6584.2001.tb02327.x>.
- WFD, 2000. *Water Framework Directive*. Retrieved from: <https://eur-lex.europa.eu/lega1-content/EN/TXT/?uri=CELEX:32000L0060>.
- WHO, 2017. *Guidelines for Drinking-Water Quality, 4th Edition, Incorporating the 1st Addendum*. World Health Organization, Geneva, 641 pp. ISBN: 978-92-4-154995-0.
- Wilkie, J.A., Hering, J.G., 1998. Rapid oxidation of geothermal arsenic(III) in streamwaters of the eastern Sierra Nevada. *Environ. Sci. Technol.* 32 (5), 657–662. <https://doi.org/10.1021/es970637r>.
- Williams, M., 2001. Arsenic in mine waters: an international study. *Environ. Earth Sci.* 40 (3), 267–278. <https://doi.org/10.1007/s002540000162>.